

## Making complex scaling work for long-range potentials

T. N. Rescigno

*Physics and Space Technology Directorate, Lawrence Livermore National Laboratory, Livermore, California 94550*

M. Baertschy and D. Byrum

*Department of Applied Science, University of California, Davis, Livermore, California 94550*

C. W. McCurdy

*Computing Sciences Directorate, Lawrence Berkeley National Laboratory, Berkeley, California 94720*

(Received 23 December 1996)

We examine finite basis set implementations of complex scaling procedures for computing scattering amplitudes and cross sections. While ordinary complex scaling, i.e., the technique of multiplying all interparticle distances in the Hamiltonian by a complex phase factor, is known to provide convergent cross-section expressions only for exponentially bounded potentials, we propose a generalization, based on Simon's exterior complex scaling technique, that works for long-range potentials as well. We establish an equivalence between a class of complex scaling transformations carried out on the time-independent Schrödinger equation and a procedure commonly referred to as the method of complex basis functions. The procedure is illustrated with a numerical example. [S1050-2947(97)07406-4]

PACS number(s): 34.80.Bm, 03.65.Nk

### I. INTRODUCTION

The method of complex coordinates or complex scaling (i.e., the idea of treating the Hamiltonian as a function of complex position variables) is well known in physics. The idea was first used over 30 years ago in the theory of potential scattering to extend the region of analyticity of the Jost function into the lower half  $k$  plane [1]. It also has a long history in atomic and molecular physics as the basis for various methods used in computational scattering theory dating back to the early seventies [2,3]. Most of the applications have centered on the calculation of resonances in atoms and molecules whose energies and lifetimes, under complex scaling, are related to the real and imaginary parts of the discrete eigenvalues of an analytically continued Hamiltonian [4]. Nevertheless, as Reinhardt pointed out in his 1982 review [5], it is important to bear in mind that the original motivation for interest in the method, and indeed the principal motivation for this study, was the prospect of calculating scattering cross sections without explicit enforcement of asymptotic boundary conditions. In contrast to the development of "direct" methods for evaluating resonances based on complex scaling [6], this other aspect has received far less attention [7,8] and, apart from applications to photoionization [9–12], has met with only partial success. The reason? A solution of the full scattering problem requires matrix elements of the resolvent between continuum functions. Unfortunately, the method of complex scaling as originally presented only provides convergent expressions for these quantities in the case of interaction potentials that fall off exponentially [2,13], which would appear to exclude most of the problems encountered in atomic and molecular physics. Although methods based on complex scaling or, more accurately, on the use of complex basis functions [8] have been proposed to tackle this harder problem, it is probably fair to say that, after many years, no definitive method for entirely

circumventing the specification of boundary conditions has emerged.

One notable extension of the complex coordinate method was Simon's exterior complex scaling procedure [14], in which the coordinates are only scaled outside a (hyper)sphere of radius  $|\mathbf{r}|=R_0$ . The motivation for this development was the desire to treat Hamiltonians that have nonanalyticities in the interior region, such as the Born-Oppenheimer Hamiltonian whose electron-nuclear attraction terms are not dilatation analytic when viewed solely as a function of the electronic coordinates [15]. In computational applications, exterior complex scaling has been used mainly in direct numerical integration methods [16–18], although there have been a few attempts, in connection with resonance evaluations, to implement the method in a basis [19–21].

The purpose of this paper is to show that exterior scaling can be used to formulate a procedure for solving the full scattering problem using only square-integrable functions and that, unlike the original complex scaling method, the method is not restricted to exponentially bounded potentials. To be able to implement the method with arbitrary basis functions, we have found it necessary to generalize Simon's procedure to a broader class of transformations, where the transition from real to scaled coordinates is smoothly carried out over a finite range.

The method is outlined in the following sections, after a brief review of the earlier techniques. We then make some comments on the connection between complex scaling and complex basis function methods. Section V presents some numerical examples and Sec. VI has some concluding remarks.

### II. COMPLEX SCALING

For notational simplicity, we will use the symbol  $r$  to refer collectively to all the interparticle coordinates in an

$N$ -body system. The starting point for a definition of the complex coordinate method is to introduce a scaling of  $r$  by a real factor  $e^\theta \in \mathbb{R}$  under which the wave function is mapped as

$$\Psi(r) \rightarrow e^{N\theta/2} \Psi(e^\theta r), \quad (1)$$

where the factor  $e^{N\theta/2}$  must be included to preserve the normalization of the wave function. Since  $\theta$  is real, this corresponds to a unitary transformation of the Hamiltonian,  $H_\theta = U(\theta) H U^{-1}(\theta)$ , and the spectrum of  $H_\theta$  is independent of  $\theta$ .

The complex coordinate method analytically continues  $H_\theta$  by considering a broader class of (nonunitary) scaling transformations  $e^\theta, \theta \in \mathbb{C}$ . In this paper, we use the terms ‘‘uniform’’ or ‘‘ordinary’’ complex scaling to denote this transformation which scales all interparticle coordinates by a complex constant. There is a considerable literature on the properties of the Hamiltonian under this (nonunitary) transformation for the class of *dilatation analytic* potentials [5,22], the principal results of which can be summarized as follows.

(1) The bound-state eigenvalues of  $H_\theta$  are the same as those of  $H$  for  $|\arg \theta| \leq \pi/2$ .

(2) The segments of the continuous spectrum of  $H_\theta$  beginning at each scattering threshold are rotated into the lower half plane by an angle  $2 \operatorname{Im} \theta$  ( $\operatorname{Im} \theta > 0$ ).

(3)  $H_\theta$  may have isolated complex eigenvalues (resonances), and corresponding  $L^2$  eigenfunctions, in the wedge formed by the continuous spectra of  $H$  and  $H_\theta$ . They are independent of  $\theta$  as long as they are not covered by branches of the continuous spectrum of  $H_\theta$ .

Property 3 has accounted for the attractiveness of uniform complex scaling as a means for finding resonances. Consider, for example, the case of  $s$ -wave scattering from a spherically symmetric potential  $V(r)$ . One simply chooses a basis of  $L^2$  functions, forms a (complex symmetric) matrix representation of the operator

$$H_\theta(r) = -\frac{1}{2} e^{-2\theta} \frac{d^2}{dr^2} + V(re^\theta), \quad (2)$$

diagonalizes it and varies  $\theta$  to find those eigenvalues which are roughly independent of the scaling angle. In practice, the eigenvalues may depend strongly on the rotation angle for basis sets that are not carefully optimized and modifications of the method, which need not concern us here, are needed to make the method practical for many-electron systems [23]. We refer the interested reader to several reviews for further details [5,6,24].

It is property 2 that has stimulated interest in complex scaling as a way to implement scattering theories that do not rely on explicit enforcement of asymptotic boundary conditions. The idea is to express the quantity of interest, such as a scattering amplitude, as a matrix element of the resolvent or full Green’s function  $\lim_{\varepsilon \rightarrow 0} (E - H + i\varepsilon)^{-1}$  and to use the fact that the latter can be approximated as the inverse of the matrix representation of  $E - H_\theta$  in an  $L^2$  basis, i.e., as  $(\tilde{E} - \tilde{H}_\theta)^{-1}$  [2,8]. Because the continuous spectrum of  $H_\theta$  has been rotated off the real axis, the matrix  $(\tilde{E} - \tilde{H}_\theta)^{-1}$  is a meaningful approximation to the resolvent for real values of

$E$ . To evaluate the scattering amplitude or  $T$  matrix, we require matrix elements of the resolvent between continuum functions. Specifically, what is required is  $\lim_{\varepsilon \rightarrow 0} \langle \psi_0 | V (E - H + i\varepsilon)^{-1} V | \psi_0 \rangle$ , where  $\psi_0$  is a continuum function. Unfortunately, with ordinary complex scaling, these so-called ‘‘free-free’’ elements only converge for exponentially bounded potentials  $V$  [2,13]. Our main purpose here will be to show how such a construction can be made to work even in the case of a Hamiltonian with long-range interactions.

The method of exterior complex scaling was proposed by Simon [14] as a logical extension of uniform complex scaling to deal with potentials that may have interior nonanalyticities, but are well behaved outside some (hyper)sphere of finite volume [25]. Specifically, Simon suggested the mapping

$$Q_{R_0, \phi}(r) = \begin{cases} r, & r < 0 \\ R_0 + (r - R_0) e^{i\phi}, & r \geq R_0 \end{cases} \quad (3)$$

The spectral properties of the Hamiltonian under this more general scaling transformation are the same as those listed above for uniform complex scaling. The particular example that prompted Simon’s work was the Born-Oppenheimer Hamiltonian with fixed, real nuclear coordinates. The nonanalyticity of the electron-nuclear attraction terms spell trouble for uniform scaling [15], but are readily accommodated under exterior complex scaling.

The slope of the contour defined by Simon’s exterior complex scaling changes discontinuously at  $R_0$ , which can complicate its implementation in certain applications [26]. We will therefore first consider a more general class of transformations which pass smoothly from real to complex  $r$  and then return to exterior complex scaling as a limiting case. We will use the term smooth exterior scaling to distinguish this class of mappings from Simon’s original prescription, which we call sharp exterior scaling, while the term ‘‘complex scaling’’ without modifiers can refer to any method which allows the position variables to take on complex values.

Consider some smooth complex contour  $R(r)$  which has the properties

$$R(r) = \begin{cases} r, & r \rightarrow 0 \\ r e^{i\phi}, & r \rightarrow \infty \end{cases} \quad (4)$$

but is otherwise arbitrary. We first need to determine the explicit form of the transformed Schrödinger equation as a function of the real coordinate  $r$ .

The implementation of complex scaling requires that one take into account the metric which accompanies the scaling operator. In analogy with Eq. (1), we define the operator that does the scaling as

$$U \Psi(r) = J(r) \Psi(R(r)), \quad (5)$$

where the Jacobian is

$$J(r) = \left( \frac{dR}{dr} \right)^{1/2} \quad (6)$$

and the scaled Schrödinger equation is

$$U H U^{-1} U \Psi = E U \Psi. \quad (7)$$

The inverse of  $U$  is given by

$$U^{-1}\Psi = \frac{1}{J(R^{-1}(r))} \Psi(R^{-1}(r)), \quad (8)$$

where  $R^{-1}(r)$  is the inverse of the function defining the contour.

Next, we need an expression for the radial kinetic-energy operator under this transformation. The algebra simplifies considerably if we represent the contour in the following form [26]:

$$R(r) = \int_0^r q(r') dr', \quad (9)$$

with

$$q(r) = \begin{cases} 1, & r \rightarrow 0 \\ e^{i\phi}, & r \rightarrow \infty \end{cases} \quad (10)$$

so that

$$J(r) = q^{1/2}(r) \quad (11)$$

for functions  $q$  that are continuous. Finally, if we define  $\varphi(r)$  as the original wave function on the contour, i.e.,

$$U\Psi(r) \equiv J(r)\varphi(r) = q^{1/2}(r)\varphi(r), \quad (12)$$

then it can be shown that

$$U \frac{d^2}{dr^2} U^{-1}(r) q^{1/2}(r) \varphi(r) = \frac{1}{q^2} q^{1/2} \varphi'' - \frac{q'}{q^3} q^{1/2} \varphi', \quad (13)$$

where the primes denote differentiation with respect to the real coordinate  $r$ . The transformed radial Schrödinger equation  $\hat{H}\varphi(r) = E\varphi(r)$  involves the Hamiltonian operator

$$\hat{H}(r) = -\frac{1}{2} \left[ \frac{1}{q^2} \frac{d^2}{dr^2} - \frac{q'}{q^3} \frac{d}{dr} \right] + V(R(r)). \quad (14)$$

This representation of the second derivative operator now allows us to derive a symmetric matrix representation of the scaled Schrödinger equation in a basis. The idea is to expand just  $\varphi(r) \equiv \Psi(R(r))$ , and not  $U\Psi(r)$  which contains the Jacobian factor, in a basis

$$\varphi(r) = \sum_n C_n \chi_n(r). \quad (15)$$

Inserting this expression into Eq. (14), multiplying from the left with  $q(r)\chi_m(r)$  and integrating over  $r$  gives

$$\sum_n \tilde{H}_{mn} C_n = E \sum_n \tilde{S}_{mn} C_n, \quad (16)$$

with

$$\tilde{S}_{mn} = \int_0^\infty \chi_m(r) \chi_n(r) q(r) dr, \quad (17)$$

$$\tilde{H}_{mn} = \tilde{T}_{mn} + \tilde{V}_{mn}, \quad (18)$$

$$\tilde{V}_{mn} = \int_0^\infty \chi_m(r) V(R(r)) \chi_n(r) q(r) dr, \quad (19)$$

$$\tilde{T}_{mn} = -\frac{1}{2} \int_0^\infty \chi_m(r) \left[ \frac{1}{q(r)} \chi_n''(r) - \frac{q'(r)}{q^2(r)} \chi_n'(r) \right] dr, \quad (20a)$$

$$= \frac{1}{2} \int_0^\infty \chi_m'(r) \frac{1}{q(r)} \chi_n'(r) dr, \quad (20b)$$

where the last expression comes from integration by parts and the assumption that the basis functions vanish at the origin and infinity. Note that the kinetic-energy elements given by Eq. (20b) obviously define a *complex symmetric* matrix.

Equations (17)–(20) which, together with the transformed Hamiltonian in Eq. (14), are the principal results of this section, show how to represent the transformed radial Schrödinger equation in a basis. In the limiting case of sharp exterior scaling,  $q(r)$  changes discontinuously from 1 to  $e^{i\phi}$  at  $r = R_0$  and some care is needed to properly define the kinetic-energy elements. It can be shown that Eq. (20b) still gives the correct representation of the kinetic-energy operator in this instance. Note that, unlike Kurasov, Scrinzi, and Elander [26], we have not included the Jacobian factor  $\sqrt{q(r)}$  in the definition of the scaled wave function in Eq. (5) so that, under sharp exterior scaling,  $\Psi(R(r))$  is *not* discontinuous at  $R_0$ . However, the derivatives of  $\Psi(R(r))$  (with respect to  $r$ ) are discontinuous. The implication is that, even with the kinetic-energy operator properly defined via Eq. (20b), an analytic basis set cannot give uniform convergence with sharp exterior scaling because such an expansion cannot represent the cusp discontinuity in the wave function at  $R_0$ .

### III. COMPLEX SCALING VS COMPLEX BASIS FUNCTIONS

At this point, it is possible to establish a connection between complex scaling and another class of techniques commonly referred to as complex basis function methods. For some implementations of complex scaling, it is possible to reinterpret the prescription of using real  $L^2$  functions in connection with a complex Hamiltonian as being entirely equivalent to using complex basis functions with a real Hamiltonian. For example, with uniform scaling, we have  $q(r) = e^{i\phi} \forall r$  and thus have to construct matrix elements of the form

$$I = e^{i\phi} \int_0^\infty \chi_m(r) H(re^{i\phi}) \chi_n(r) dr. \quad (21)$$

It is easy to see that if we make the change of variable  $r \rightarrow re^{-i\phi}$  in the above integral and use Cauchy's theorem to distort the integration contour back to the real axis, we get

$$I = \int_0^\infty \chi_m(re^{-i\phi}) H(r) \chi_n(re^{-i\phi}) dr, \quad (22)$$

so that we can view the case of uniform scaling as being equivalent to using a real Hamiltonian and working with

complex basis functions  $\chi_n(re^{-i\phi})$  and a scalar product defined without complex conjugation of the radial functions. While complex scaling and complex basis functions are equivalent in this simple case, the complex basis function interpretation turned out to be more flexible, since it allowed one to mix real and complex basis functions in many-body problems where the wave functions are represented as orbital products. The inner-core orbitals in a heavy atom become highly oscillatory under uniform complex scaling which causes severe convergence problems. With complex basis function methods, one can use real basis functions to expand the core orbitals and complex functions only for the outer orbitals [23]. The method is then no longer the same as uniform complex scaling and may well not correspond to an easily derived variable scaling of the Hamiltonian operator. The ‘‘method of complex basis functions’’ [23,24] played an important role in the evolution of numerical scattering methods, since it enabled practical calculations to be performed on many-electron atoms as well as molecules. In fact, some progress was made in establishing a relationship (but not an identity) between computations carried out with complex basis functions and the exterior complex scaling concept [27].

The development of the preceding section enables us to make a clearer connection between complex scaling and complex basis functions. The matrix elements we have to consider [Eqs. (17), (19), and (20)] have the form

$$\begin{aligned}\tilde{H}_{mn} &= \int_0^\infty \chi_m(r)H(R(r))\chi_n(r)q(r)dr \\ &= \int_0^\infty \chi_m(r)H(R(r))\chi_n(r) \frac{dR}{dr} dr.\end{aligned}\quad (23)$$

If we can construct  $R^{-1}$ , the inverse of the function which defines the contour, then we can make the change of variable from  $r$  to  $x$ , where  $r=R^{-1}(x)$  and again use Cauchy’s theorem to carry out the integration along the real  $x$  axis. The result is

$$\tilde{H}_{mn} = \int_0^\infty \chi_m(R^{-1}(x))H(x)\chi_n(R^{-1}(x))dx, \quad (24)$$

which establishes the desired connection between complex scaling and an equivalent complex basis. For the case of uniform complex scaling, as well as sharp exterior scaling, the inverse map is simply  $R^{-1}(r)=r^*$ . In fact, any smooth mapping that satisfies

$$R^{-1}(x) = \begin{cases} x, & x \rightarrow 0 \\ xe^{-i\phi}, & x \rightarrow \infty \end{cases} \quad (25)$$

and has a smooth inverse can be used to define a set of complex basis functions to use in Eq. (24). Note that with exterior scaling, there is no need for mixing real and complex basis functions; the inner-core orbital problem in many-electron systems is automatically handled in a natural way, since tight functions that do not extend beyond  $R_0$  are effectively left real.

#### IV. SCATTERING

We will next investigate the question of applying the formalism outlined above to a collision problem. For simplicity, we will consider the case of  $s$ -wave scattering from a spherically symmetric potential. The scattering cross section is proportional to the squared modulus of the  $T$  matrix, which is defined as

$$\begin{aligned}T(E) &= \int_0^\infty \psi_0(r)V(r)\psi^\dagger(r)dr \\ &\equiv \int_0^\infty \psi_0(r)V(r)(\psi_0(r) + \psi^{\text{scat}}(r))dr,\end{aligned}\quad (26)$$

where  $\psi^{\text{scat}}(r)$  is the scattered wave part of the full scattering wave function. The  $T$  matrix can also be expressed in terms of the full Green’s function

$$\begin{aligned}T(E) &= \int_0^\infty \psi_0(r)(V(r) + V(r)G^+(r,r')V(r'))\psi_0(r)dr dr' \\ &= \lim_{\epsilon \rightarrow 0} \langle \psi_0 | V + V(E + i\epsilon - H)^{-1}V | \psi_0 \rangle,\end{aligned}\quad (27)$$

with

$$\psi_0 = \sqrt{2/k} \sin(kr), \quad E = k^2/2. \quad (28)$$

Note that with these definitions,  $T = e^{i\delta} \sin \delta$ , where  $\delta$  is the phase shift. The scattered wave part of the  $T$ -matrix is now approximated as

$$\langle \psi_0 | V(E + i\epsilon - H)^{-1}V | \psi_0 \rangle \approx \bar{f} \cdot (E\tilde{S} - \tilde{H}_\theta)^{-1} \cdot \bar{f}, \quad (29)$$

where the matrices  $\tilde{S}$  and  $\tilde{H}$  are defined in Eqs. (17)–(20) and  $\bar{f}$  is a vector with elements

$$f_m = \sqrt{2/k} \int_0^\infty \chi_m(r)V(R(r))\sin(kR(r))q(r)dr, \quad (30)$$

Since the continuous spectrum of  $H_\theta$  has been rotated into the lower half plane, this representation should converge for real  $E$  if  $V$  is sufficiently well behaved. Unfortunately, as Baumel, Crocker, and Nuttall [13] have pointed out,  $V(r)$  must be exponentially bounded for Eq. (29) to converge since  $\sin(kr)$  diverges exponentially under coordinate rotation. This will be formally true both for uniform scaling or exterior scaling. With exterior complex scaling, however, there is a way around this problem.

Although the development to this point allows any switching function  $q(r)$  that satisfies Eq. (10), we will see that there are distinct advantages to having a contour that coincides *exactly* with the real axis over a finite range  $0 \leq r \leq R_0$ . We can then replace the original potential  $V(r)$  by a finite range potential  $V_{R_0}(r)$  that vanishes beyond  $R_0$  and is identical to  $V(r)$  for  $r < R_0$

$$V_{R_0}(r) = \begin{cases} V(r), & r \leq R_0 \\ 0, & r > R_0 \end{cases}. \quad (31)$$

We can use exterior scaling to calculate the  $T$  matrix corresponding to this potential  $T_{R_0}$  relying on Eq. (29) to approxi-

mate the scattered wave part in a basis set of  $N$  square-integrable functions with Eqs. (17)–(20) defining the required matrix elements. Since  $V_{R_0}(r)$  is a finite-range potential, the method will converge for any value of  $R_0$  if  $N$  is large enough. This truncation of the potential allows us to define a process that limits to the correct physical result as  $R_0 \rightarrow \infty$ . Thus, by choosing the *interior* region large enough, we can insure that the truncated potential differs insignificantly from the physical potential under consideration [28].

We can contrast the above procedure to the situation that pertains to uniform complex scaling with a truncated long-range potential. In the latter case, it is convenient to use the ‘‘complex basis set’’ interpretation of uniform scaling [i.e., Eq. (22)], so that we can continue to use the same real, finite-range potential  $V_{R_0}(r)$ . The matrix elements of the potential would then be of the form

$$I_{R_0} = \int_0^{R_0} \chi_m(re^{-i\phi})V(r)\chi_n(re^{-i\phi})dr. \quad (32)$$

In contrast to the case of exterior scaling with  $V_{R_0}(r)$ , uniform scaling will not yield physically meaningful results as  $R_0$  is increased. Indeed, in the limit  $R_0 \rightarrow \infty$ , the matrix elements defined in Eq. (32) become, after the change of variable  $r \rightarrow re^{i\phi}$

$$I_{R_0} \lim_{R_0 \rightarrow \infty} = e^{i\phi} \int_0^\infty \chi_m(r)V(re^{i\phi})\chi_n(r)dr, \quad (33)$$

which is precisely the case that Baumel, Crocker, and Nuttall [13] showed to be divergent.

We will now give the specific form of the transformation we used to implement smooth exterior scaling. We chose

$$q(r) = \begin{cases} 1, & r < R_0 - h \\ f(r), & R_0 - h < r < R_0 + h, \\ e^{i\phi}, & r > R_0 + h \end{cases} \quad (34)$$

where  $f(r)$  is a smooth switching function defined on  $[R_0 - h < r < R_0 + h]$ . To insure uniform convergence with an analytic basis, we want  $f(r)$  to be continuously differentiable at  $r = R_0 \pm h$ . We thus chose  $f(r)$  to be the lowest order polynomial needed to make  $q(r)$  and  $q'(r)$  continuous at  $R_0 - h$  and  $R_0 + h$ . If we define

$$f(r) = 1 + (e^{i\phi} - 1)P\left(\frac{r - R_0}{h}\right), \quad (35)$$

then the requirement is that  $P(-1) = 0$ ,  $P(1) = 1$ ,  $P'(-1) = 0$  and  $P'(1) = 0$ . These conditions uniquely define  $P(x)$

$$P(x) = \frac{1}{4}(2 + 3x - x^3). \quad (36)$$

The truncated potential  $V_{R_0}$  is defined as

$$V_{R_0} = \begin{cases} V(R(r)) = V(r), & r < R_0 - h \\ 0, & r \geq R_0 - h \end{cases}. \quad (37)$$

We reiterate that by zeroing the potential on the complex portion of the contour, we eliminate any numerical difficul-

TABLE I. Phase shift for  $s$ -wave scattering by an exponential potential.  $N$  refers to the number of Laguerre-type functions used in the calculation. Results are given for both uniform complex scaling and smooth exterior scaling. See text for basis set and contour parameters.

$N$	Uniform	Smooth Exterior
$k=0.15$		
5	-0.898 511 72	-0.000 003 17
10	-1.046 153 20	0.548 948 06
15	-1.058 928 49	-0.950 252 63
20	-1.047 232 52	-1.027 465 88
25	-1.051 195 81	-1.062 783 68
30	-1.050 256 94	-1.046 716 28
35	-1.050 417 02	-1.051 224 59
40	-1.050 403 38	-1.050 281 54
45	-1.050 400 37	-1.050 404 85
50	-1.050 402 26	-1.050 406 59
55	-1.050 401 68	-1.050 400 28
60	-1.050 401 80	-1.050 402 73
$k=0.35$		
5	1.423 933 79	0.000 008 38
10	1.460 337 20	0.212 813 71
15	1.461 222 77	1.436 323 77
20	1.461 247 16	1.455 724 39
25	1.461 247 57	1.461 076 10
30	1.461 247 56	1.461 245 73
35	1.461 247 56	1.461 248 05
40	1.461 247 56	1.461 248 37
$k=0.55$		
45	1.461 247 56	1.461 248 45
50	1.461 247 56	1.461 247 59
55	1.461 247 56	1.461 247 64
60	1.461 247 56	1.461 247 59
$k=0.55$		
5	1.155 837 18	-0.000 027 24
10	1.144 127 89	0.226 360 78
15	1.144 235 25	0.922 345 22
20	1.144 234 35	1.141 723 79
25	1.144 234 36	1.142 999 29
30	1.144 234 36	1.144 086 07
35	1.144 234 36	1.144 226 53
40	1.144 234 36	1.144 232 62
45	1.144 234 36	1.144 232 18
50	1.144 234 36	1.144 234 34
55	1.144 234 36	1.144 234 16
60	1.144 234 36	1.144 234 22

ties associated with a less than exponential fall off of the potential at large distances, but have no measurable effect on the cross section.

We do not expect this remedy to come without a price. It's obvious that the basis set one chooses must have elements that extend beyond the complex turning point  $R_0$ ; if not, the eigenvalues of  $\tilde{H}_\theta$  would effectively be real and Eq. (29) would not yield a sensible result. Even for a short-ranged potential then, we expect that a larger number of

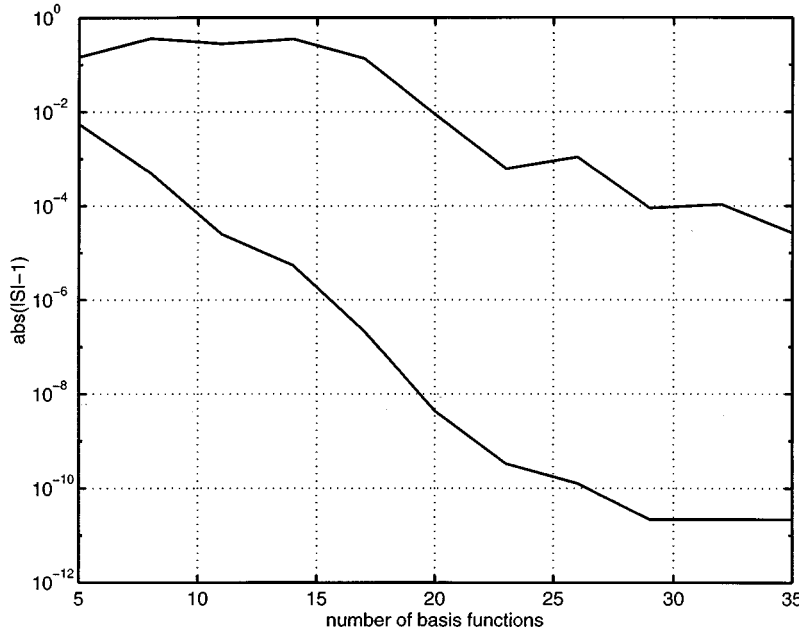


FIG. 1. Unitarity of the calculated  $S$  matrix ( $S \equiv e^{2i\delta}$ ) for  $s$ -wave scattering by an exponential potential at  $k=0.55$ . Upper curve is for smooth scaling; lower curve is for exterior scaling.

functions will be required to achieve a given level of accuracy with exterior scaling than with uniform scaling and that the number of functions required will grow as  $R_0$  increases.

We can recover Simon's original exterior complex scaling contour by letting  $h \rightarrow 0$  in Eq. (34), in which case  $q$  changes discontinuously at  $R_0$ . Equation (20b) can still be used to define the kinetic-energy matrix, but analytic basis functions will not give uniform convergence with this prescription since the derivative of the wave function (with respect to  $r$ ) is discontinuous at  $R_0$ . However, the cusp discontinuity in the wave function at the point  $R_0$  that occurs with sharp exterior scaling can be accommodated by using a nonanalytic set of basis functions that are only defined on finite intervals. The continuous variable  $r$  is replaced by a grid of nodes  $0 < r_1 < r_2 < \dots < r_n < \infty$ . Finite element basis functions  $\zeta_{i,m}(r)$  are defined to be identically zero outside a given interval

$$\zeta_{i,m}(r) = 0 \quad r \notin [r_i, r_{i+1}], \quad i = 1, \dots, n. \quad (38)$$

We use the label  $m$  to indicate the boundary conditions imposed on the basis functions at the nodes, for example, zero or unity at the right or left end of the interval. The finite element functions are then combined into a smaller set of continuous basis functions on which the Hamiltonian is projected. To accommodate exterior scaling, we simply require the point  $R_0$  to coincide with one of the nodes. To construct the required Hamiltonian matrix elements, we have to consider terms of the form

$$\begin{aligned} & \int_0^\infty \zeta_{i,m}(r) H(R(r)) \zeta_{j,n}(r) q(r) dr \\ &= \delta_{i,j} \int_{r_i}^{r_{i+1}} \zeta_{i,m}(r) H(R(r)) \zeta_{i,n}(r) \frac{dR}{dr} dr, \end{aligned} \quad (39)$$

where, by construction, the point  $R_0$  never lies *within* the interval  $[r_i, r_{i+1}]$  and, hence,  $R(r)$  is always smooth over the integration range. To underscore the fact that the finite

element basis functions depend explicitly on the interval boundaries, we write them as  $\zeta_{i,j}(r) \equiv f_j(r, r_i, r_{i+1})$ . In our implementation of the method, we used Hermite interpolating polynomials  $f_j(r, r_i, r_{i+1})$ , which are uniquely defined on the interval  $[r_i, r_{i+1}]$  from the conditions

$$\begin{aligned} \frac{d^k}{dr^k} f_j(r, r_i, r_{i+1}) &= \delta_{j,k}, \quad r = r_i, \\ \frac{d^k}{dr^k} f_j(r, r_i, r_{i+1}) &= 0, \quad r = r_{i+1}. \end{aligned} \quad (40)$$

For these functions, there is a simple proportionality between  $f_j(r, r_i, r_{i+1})$  and  $f_j(R(r), R(r_i), R(r_{i+1}))$ , where  $R(r)$  is any linear function of  $r$ . Since the exterior scaling contour is a linear transformation on  $r$ , we can thus write

$$\begin{aligned} & \int_0^\infty \zeta_{i,m}(r) H(R(r)) \zeta_{j,n}(r) q(r) dr \propto \delta_{i,j} \\ & \times \int_{R(r_i)}^{R(r_{i+1})} f_m(R(r), R(r_i), R(r_{i+1})) \\ & \times H(R(r)) f_n(R(r), R(r_i), R(r_{i+1})) dR. \end{aligned} \quad (41)$$

This relation is remarkable for two reasons. Firstly, it shows that the finite elements naturally scale onto the rotated contour and thus can handle any step discontinuity in the wave function at the point  $R_0$ . Moreover, if analytic forms are available for the matrix elements for real intervals, then the right-hand side of Eq. (41) shows that those same formulas, evaluated for complex nodal points, give the correct values for the matrix elements of the Hamiltonian on the complex part of the contour. This would not be true if the turning point  $R_0$  fell between two nodes. It is important to bear in mind that the identity expressed in Eq. (41) does not in any sense represent a contour distortion of the integral defined in Eq. (39).

### V. EXAMPLES

In this section we will illustrate some of the ideas we have outlined with several numerical examples. We will first report the results of calculations using analytic basis functions on a smoothly scaled contour. To examine questions of convergence, it is convenient to work with a set of  $L^2$  functions that can be systematically increased toward completeness without running into problems of numerical linear dependence. We chose the set of functions

$$\chi_{n,\lambda}(r) = \frac{\lambda^{3/2}}{[(n+1)(n+2)]^{1/2}} r e^{-\lambda r/2} L_n^2(\lambda r), \quad (42)$$

where  $L_n^2(\lambda r)$  is an associated Laguerre polynomial. These functions are orthonormal on  $[0, \infty]$  and give simple analytic expressions for matrix elements of the  $s$ -wave kinetic energy

$$\begin{aligned} T_{m,n} &\equiv -\frac{1}{2} \int_0^\infty \chi_{m,\lambda}(r) \frac{d^2}{dr^2} \chi_{n,\lambda}(r) dr \\ &= \lambda^2 \left[ -\delta_{m,n}/8 + \frac{(2m^3 + 9m^2 + 13m + 6)}{12\sqrt{(n+1)(n+2)(m+1)(m+2)}} \right]. \end{aligned} \quad (43)$$

These analytic formulas can even be used to simplify the evaluation of matrix elements carried out on a complex contour where numerical quadrature is required, i.e., where we use

$$\begin{aligned} &\int \chi_{m,\lambda}(r) H(R(r)) \chi_{n,\lambda}(r) q(r) dr \\ &\approx \sum_i \chi_{m,\lambda}(r_i) H(R(r_i)) \chi_{n,\lambda}(r_i) q(r_i) w_i. \end{aligned} \quad (44)$$

We can make use of the fact that  $q(r) = e^{i\phi}$  for  $r > R_0 + h$  to simplify evaluation of the overlap and kinetic-energy matrix elements. In the case of the overlap matrix, for example, we write

$$\begin{aligned} &\int_0^\infty \chi_{m,\lambda}(r) \chi_{n,\lambda}(r) q(r) dr \\ &= \int_0^{R_0+h} \chi_{m,\lambda}(r) \chi_{n,\lambda}(r) q(r) dr + e^{i\phi} \left[ \int_0^\infty \chi_{m,\lambda}(r) \right. \\ &\quad \left. \times \chi_{n,\lambda}(r) dr - \int_0^{R_0+h} \chi_{m,\lambda}(r) \chi_{n,\lambda}(r) dr \right] \\ &\approx e^{i\phi} \delta_{m,n} + \sum_j \chi_{m,\lambda}(r_j) \chi_{n,\lambda}(r_j) (q(r_j) - e^{i\phi}) w_j, \end{aligned} \quad (45)$$

where the quadrature points only cover the interval  $[0, R_0 + h]$ .

We first considered  $s$ -wave scattering from the short-range potential

$$V(r) = -e^{-r} \quad (46)$$

TABLE II. Phase shift for  $s$ -wave scattering by truncated long range potential.  $N$  refers to the number of Laguerre-type functions used in a smooth exterior scaling calculation. See text for basis set and contour parameters.

$N$	$R_0=25$	$R_0=35$
	$k=0.15$	
10	-0.010 800 94	-0.000 000 15
20	-0.069 561 68	-0.164 917 53
30	-0.060 820 42	-0.061 410 67
40	-0.060 917 40	-0.060 926 53
50	-0.060 944 40	-0.061 025 23
60	-0.060 945 59	-0.061 030 83
70	-0.060 945 56	-0.061 030 78
80	-0.060 945 58	-0.061 030 78
90	-0.060 945 59	-0.061 030 79
100	-0.060 945 59	-0.061 030 78
	$k=0.35$	
10	-0.000 384 21	-0.000 000 01
20	-0.099 657 09	-0.037 669 36
30	-0.100 319 07	-0.100 177 26
40	-0.100 336 19	-0.100 404 43
50	-0.100 336 28	-0.100 411 17
60	-0.100 336 39	-0.100 410 98
70	-0.100 336 48	-0.100 410 97
80	-0.100 336 48	-0.100 410 97
90	-0.100 336 48	-0.100 411 06
100	-0.100 336 49	-0.100 411 09
	$k=0.55$	
10	-0.000 361 34	-0.000 000 01
20	-0.132 563 05	-0.043 013 91
30	-0.118 845 09	-0.114 737 08
40	-0.118 665 69	-0.118 511 86
50	-0.118 658 89	-0.118 669 29
60	-0.118 658 68	-0.118 689 69
70	-0.118 658 54	-0.118 691 13
80	-0.118 658 59	-0.118 691 33
90	-0.118 658 57	-0.118 691 37
100	-0.118 658 56	-0.118 691 29

and compared the results obtained from uniform complex scaling, i.e.,  $H(r) \rightarrow H(re^{i\phi})$ , with smooth exterior scaling  $H(r) \rightarrow H(R(r))$ . The contour used the polynomial switching function described in Sec. IV. For these calculations, we chose  $R_0 = 20.0$  and  $h = 4.0$ . The Laguerre scale factor  $\lambda$  was set to 2.0 and the rotation angle was  $30^\circ$  for both sets of calculations. Table I shows the behavior of the  $s$ -wave phase shift (defined here as the phase of the calculated  $T$  matrix) for several values of  $k$ . The convergence is faster with uniform scaling than with smooth exterior scaling, as we conjectured, because with smooth exterior scaling one first needs to span the region from the origin to  $R_0$  before one begins to see convergence. This can be seen in Fig. 1, which compares uniform and smooth exterior scaling for  $k = 0.55$ . The measure of convergence for this comparison is the unitarity of the  $S$  matrix ( $S = e^{2i\delta}$ ), which is computed from the  $T$  matrix as  $S = 1 + 2iT$ .

The next case we consider is  $s$ -wave scattering from the long-range potential

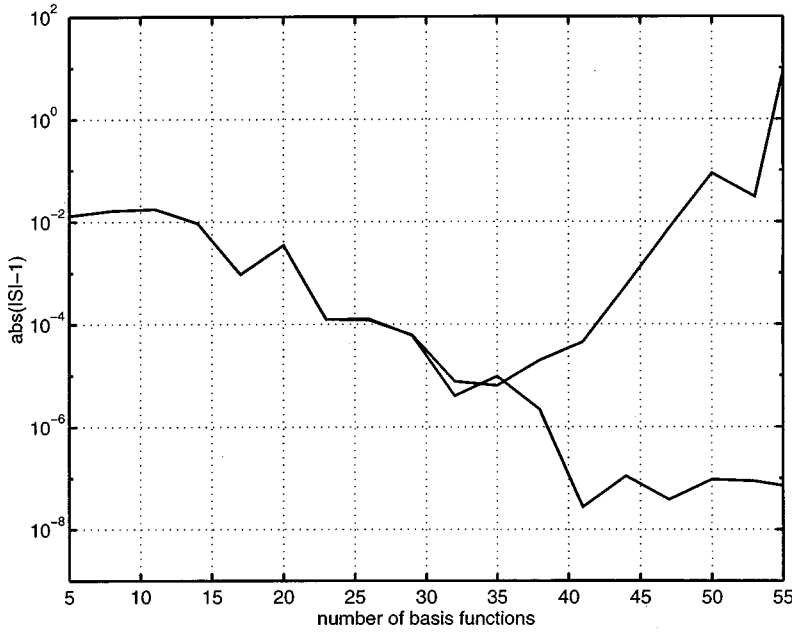


FIG. 2. Unitarity of the calculated  $S$  matrix ( $S \equiv e^{2i\delta}$ ) for  $s$ -wave scattering by a long-range potential at  $k=0.55$ . The divergent upper curve is for a potential which is not truncated on the complex part of the integration contour.

$$V(r) = \frac{1}{(1+r)^4}, \quad (47)$$

for which uniform complex scaling diverges. We again studied convergence with the smooth exterior scaling transformation, this time zeroing the potential beyond  $R_0 - h$ , where the contour begins to turn off the real axis. Results are shown in Table II for several  $k$  values and two different values of  $R_0$ . All other parameters of the contour and basis are the same as in the preceding case. The rate of convergence is similar to what was found with the exponential potential, but the converged phase shifts show a slight dependence on  $R_0$ , reflecting their dependence on the point beyond which the potential is truncated. For comparison, we also show, in Fig. 2, the results of a calculation in which the long-range potential is not truncated. It is noteworthy that calculations using the untruncated potential can provide useful results for a range of basis set values, before they ultimately begin to diverge.

We also implemented sharp exterior scaling in a finite element basis of fifth-order Hermite interpolating polynomials. In each interval  $[r_i, r_{i+1}]$ , we can uniquely define six independent polynomials  $P_{j,i}(r)$  and  $Q_{j,i}(r)$ ,  $j=0,1,2$  from the conditions

$$\begin{aligned} \frac{d^k}{dr^k} P_{j,i}(r_i) &= \delta_{j,k} \\ \frac{d^k}{dr^k} P_{j,i}(r_{i+1}) &= 0 \\ \frac{d^k}{dr^k} Q_{j,i}(r_{i+1}) &= \delta_{j,k} \\ \frac{d^k}{dr^k} Q_{j,i}(r_i) &= 0 \end{aligned}, \quad j, k = 0, 1, 2 \quad (48)$$

The explicit formulas for the  $P_{j,i}$  are

$$P_{0,i}(r) = \left( \frac{r-r_{i+1}}{r_i-r_{i+1}} \right)^3 \left[ 6 \left( \frac{r-r_{i+1}}{r_i-r_{i+1}} \right)^2 - 15 \left( \frac{r-r_{i+1}}{r_i-r_{i+1}} \right) + 10 \right],$$

$$P_{1,i}(r) = (r_{i+1}-r_i) \left( \frac{r-r_{i+1}}{r_i-r_{i+1}} \right)^2 \left[ 3 \left( \frac{r-r_{i+1}}{r_i-r_{i+1}} \right)^2 - 7 \left( \frac{r-r_{i+1}}{r_i-r_{i+1}} \right) + 4 \right],$$

$$P_{2,i}(r) = \frac{1}{2} (r_i-r_{i+1})^2 \left( \frac{r-r_{i+1}}{r_i-r_{i+1}} \right)^3 \left[ \left( \frac{r-r_{i+1}}{r_i-r_{i+1}} \right) - 1 \right], \quad (49)$$

for  $r_i \leq r \leq r_{i+1}$  and zero elsewhere. The functions  $Q_{j,i}$  are obtained by interchanging  $r_i$  and  $r_{i+1}$  in the formulas for  $P_{j,i}$ .

We can use these polynomials to define three basis functions at each node  $r_i$  which span the interval  $[r_{i-1}, r_{i+1}]$ , and have vanishing value, first and second derivative at the end points. The basis functions are defined as

$$\chi_{j,i}(r) \equiv (P_{j,i}(r) + Q_{j,i-1}(r)) \quad (50)$$

and are plotted in Fig. 3. It is obvious from Eq. (49) that the basis functions defined in Eq. (50) scale onto the contour as described in Sec. IV. In particular, at the point  $r_i = R_0$ , we see that

$$\lim_{\varepsilon \rightarrow 0} (\chi_{j,i}(R_0 + \varepsilon)) = (e^{i\phi})^j \chi_{j,i}(R_0 - \varepsilon). \quad (51)$$

Thus the function  $\chi_{0,i}$  guarantees continuity of the wave function at  $r_i = R_0$ , while  $\chi_{1,i}$  and  $\chi_{2,i}$  impose the proper discontinuity conditions on the first and second derivatives, respectively. To impose boundary conditions that the wave function vanish at the origin and last grid point, we simply omit the functions  $\chi_{0,1}$  and  $\chi_{0,N}$  and remove  $P_{j,1}$  and  $Q_{j,N}$ ,  $j=1,2$  from the definition of the basis functions.



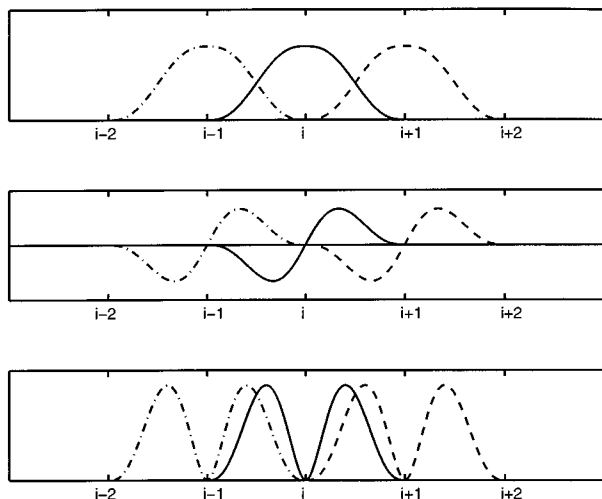


FIG. 3. Basis functions for finite element calculations. Upper panel:  $\chi_{j,0}$ ; center panel:  $\chi_{j,1}$ ; lower panel:  $\chi_{j,2}$ . See text for definition of the functions.

The exterior scaled finite element method was also applied to the long-range potential problem previously considered. For these calculations, the grid points were evenly spaced from 0 to  $r_N=100$  with  $R_0$  fixed at 25 and the rotation angle was set at  $20^\circ$ . Once again, the potential was set equal to zero along the complex portion of the contour. Table III shows the behavior of the computed phase shifts at several energies as a function of the grid spacing. Evidently, the method converges very rapidly.

## VII. DISCUSSION

We have shown that, with exterior complex scaling, we can answer the question posed by the title of this paper in the affirmative. Exterior complex scaling was originally introduced as a generalization of uniform complex scaling to deal with potentials that suffered interior nonanalyticities, but were analytic outside a sphere of finite radius. What we have shown is that by making this radius large enough so that the

TABLE III. Phase shift for  $s$ -wave scattering by truncated long-range potential. Results from exterior scaling calculations using finite elements.

Nodal spacing	$k=0.35$	$k=0.55$
12.5	-0.099 959 82	-0.104 554 62
5.0	-0.100 403 13	-0.118 680 40
2.0	-0.100 394 47	-0.118 675 91
1.0	-0.100 391 89	-0.118 673 24
0.5	-0.100 396 82	-0.118 673 16
0.25	-0.100 396 82	-0.118 673 16

potential can be truncated at this distance without physical consequence, then exterior scaling can be implemented in an  $L^2$  basis and provides a method for solving the full scattering problem without explicitly enforcing asymptotic boundary conditions, even in cases involving long-range potentials where uniform scaling diverges. For analytic basis functions, we use smooth exterior scaling to assure uniform convergence; for sharp exterior scaling, finite element basis sets can be employed. These developments allow the method to be applied to the kinds of nonresonant scattering problems encountered in atomic and molecular physics. The fact that the interaction region is represented in real coordinates also obviates the need for the mixtures of real and complex basis functions that have previously been used to treat many-electron systems. We can also show that the present development allows us to make contact with other formulations of scattering in which cross sections are evaluated by calculating the flux through a surface outside the interaction region. This will be the subject of another study.

## ACKNOWLEDGMENTS

This work was performed under the auspices of the U.S. Department of Energy by the Lawrence Livermore National Laboratory under Contract No. W-7405-Eng-48. Computer time was supplied by the National Energy Research Scientific Computing Center.

- [1] T. Regge, *Nuovo Cimento* **14**, 951 (1959); **18**, 947 (1960).  
 [2] J. Nuttall and H. L. Cohen, *Phys. Rev.* **188**, 1542 (1969).  
 [3] T. N. Rescigno and W. P. Reinhardt, *Phys. Rev. A* **8**, 2828 (1973); **10**, 158 (1974).  
 [4] G. Doolen, J. Nuttall, and R. Stagat, *Phys. Rev. A* **10**, 1612 (1974).  
 [5] W. P. Reinhardt, *Ann. Rev. Phys. Chem.* **33**, 223 (1982).  
 [6] C. W. McCurdy, in *Resonances in Electron-Molecule Scattering, van der Waal Complexes and Reactive Chemical Dynamics*, edited by D. G. Truhlar (American Chemical Society, Washington, D.C., 1984), Vol. 263, p. 17.  
 [7] B. R. Johnson and W. P. Reinhardt, *Phys. Rev. A* **28**, 1930 (1983); **29**, 2933 (1984).  
 [8] T. N. Rescigno and C. W. McCurdy, *Phys. Rev. A* **31**, 624 (1985); *Chem. Phys. Lett.* **140**, 232 (1987).  
 [9] T. N. Rescigno and V. McKoy, *Phys. Rev. A* **12**, 522 (1975).  
 [10] C. W. McCurdy and T. N. Rescigno, *Phys. Rev. A* **21**, 1499 (1980).  
 [11] T. N. Rescigno, *Phys. Rev. A* **31**, 607 (1984).  
 [12] S. Yabushita, C. W. McCurdy, and T. N. Rescigno, *Phys. Rev. A* **36**, 3146 (1987).  
 [13] R. T. Baumel, M. C. Crocker, and J. Nuttall, *Phys. Rev. A* **12**, 486 (1975).  
 [14] B. Simon, *Phys. Lett. A* **71**, 211 (1979).  
 [15] C. W. McCurdy and T. N. Rescigno, *Phys. Rev. Lett.* **41**, 14364 (1978).  
 [16] J. Turner and C. W. McCurdy, *Chem. Phys.* **71**, 127 (1982); C. W. McCurdy, C. K. Stroud, and M. K. Wisinski, *Phys. Rev. A* **43**, 5980 (1991).  
 [17] M. Rittby, N. Elander, and E. Brändas, *Int. J. Quantum Chem.* **23**, 865 (1983); *Chem. Phys.* **87**, 55 (1984).  
 [18] R. Lefebvre, *J. Phys. Chem.* **88**, 4839 (1984).

- [19] N. Lipkin, N. Moiseyev, and E. Brändas, *Phys. Rev. A* **40**, 549 (1989).
- [20] N. Rom, E. Engdahl, and N. Moiseyev, *J. Chem. Phys.* **93**, 3413 (1990).
- [21] A. Scrinzi and N. Elander, *J. Chem. Phys.* **98**, 3866 (1993).
- [22] E. Balslev and J. M. Combes, *Commun. Math. Phys.* **22**, 280 (1971); B. Simon, *Commun. Math. Phys.* **27**, 1 (1972).
- [23] T. N. Rescigno, C. W. McCurdy, and A. E. Orel, *Phys. Rev. A* **17**, 1931 (1978).
- [24] B. R. Junker, *Adv. At. Mol. Phys.* **18**, 207 (1982).
- [25] Although it has become customary to cite the work of Simon when discussing exterior scaling, the idea of using a path which is part real and part complex had been suggested earlier. Gyarmati and Vertse [*Nucl. Phys. A* **160**, 523 (1971)] had suggested such a path in connection with the normalization of resonance wave functions for charged systems, and similar ideas are discussed in J. Taylor, *Scattering Theory* (Wiley, New York, 1972), pp. 221 and 222.
- [26] P. B. Kurasov, A. Scrinzi, and N. Elander, *Phys. Rev. A* **49**, 5095 (1994).
- [27] C. W. McCurdy, *Phys. Rev. A* **21**, 464 (1980).
- [28] This discussion assumes that the potential falls off more rapidly than  $|1/r|$  at infinity.